Journal of Sound and Vibration (1998) **209**(3), 385–403

A MODELLING OF THE NOISE FROM SIMPLE COAXIAL JETS, PART I: WITH UNHEATED PRIMARY FLOW

M. J. Fisher and G. A. Preston

Institute of Sound and Vibration Research, University of Southampton, Southampton SO17 1BJ, England

AND

W. D. Bryce*

Bryce Research, Farnham GU9 8SB, England

(*Received* 28 *May* 1996, *and in final form* 18 *July* 1997)

The work described in this paper forms a portion of an on-going fundamental study of coaxial jet noise both statically and in flight. Three principal noise-producing regions are identified and their mean flow and turbulence characteristics classified from published data. The noise production from each region is then calculated by using single jet prediction methods for flows of similar mean velocity and turbulence profiles. The initial test of this prediction scheme has been conducted by comparison with data from an unheated, co-planar, coaxial jet configuration. The agreement, in terms of one-third octave spectral predictions, is significantly better than 1 dB over a wide range of both angle of observation and velocity ratio.

© 1998 Academic Press Limited

1. INTRODUCTION

Although bypass engines have dominated the civil aircraft market for about 20 years, the prediction of the jet noise from their coaxial exhaust flows has remained a difficult problem. There are several reasons for this situation, not least the large number of aerodynamic and geometric variables interacting in a complex manner, but at the root of the problem lies a major weakness in the quantitative understanding of the noise of even the simplest form of coaxial jet. The purpose of this paper is to try to formulate a basic noise model for coaxial jets which reflects the known aerodynamics characteristics of such jets and which could be used to improve prediction techniques for aircraft noise.

2. BACKGROUND

Forty years after the publication of Lighthill [1] of the first generally accepted theory for the noise from single-stream jets, prediction still relies heavily on empirical methods derived primarily from model-scale test data. The reasons are clear.

First, at the fundamental level, the turbulence closure problem means that even the most sophisticated C.F.D. methods cannot yield the properties of the turbulent field in the detail required for noise calculation.

* Formerly at Defence Research Agency Pyestock.

0022–460X/98/030385 + 19 $25.00/0/sv971218 © 1998 Academic Press Limited

Second, while a major attraction of the work [1] was that simple scaling laws for jet noise may be obtained with a minimal knowledge of the turbulent field, the predictions are not followed in detail by the data. In particular, the variation of spectra with angle to the jet axis are poorly predicted, particularly for the mid to high frequencies.

It was arguably the work of Lush [2] that first revealed the systematic nature of these discrepancies as an apparent lack of the predicted convective amplification of these frequencies. This, in turn, led Lilley [3] to re-formulate the problem in a manner which more clearly separated noise generation from subsequent interaction between the acoustic waves and the flow field of the jet, essentially the process of refraction. The subsequent development of these ideas, notably the work of Morfey, Tester and Szewczyk [4, 5], did much to put the prediction (scaling) of jet noise on a rational basis in respect of both the effects of temperature (or density) and its directionality. Unfortunately, their method breaks down over a range of angles near the positive jet axis (i.e., within the cone of relative silence) when the eddy convection velocity exceeds the ambient speed of sound. The nature of the phenomenon involved is clearly demonstrated in the helium jet data of Smith and Johannessen [6]. It seems probable that the explanation is associated with supersonically convecting disturbances or Mach wave radiation; see reference [7] for example.

As a result of these difficulties, the prediction of single-stream jet noise still relies almost exclusively on systematic databases together with the empirical approaches based thereon [8–11].

The situation pertaining to dual stream or coaxial jets, of principal interest in current and future generations of aero-engines, is worse. Here, even the experimental expedient of developing a systematic database is severely limited by the number of variables involved. In addition to the values of absolute velocity and temperature required for single-stream jets, parameters such as the secondary-to-primary velocity ratio ($\lambda = V_s / V_p$), the area ratio and the temperature ratio arise, together with a wide range of possible geometric configurations describing the relative positions of the primary and secondary nozzles both axially and radially.

This fundamental difficulty might be alleviated if it were possible to construct the noise of a coaxial jet from a number of single-stream jet components. Such a technique could substantially reduce the amount of data required as a result of a greatly improved ability to interpolate between test points and could, in addition, offer a sounder basis for the development of a generalized, albeit less accurate, prediction method.

Thus the modelling of coaxial jet noise became the objective of a research study. The component aerodynamic structure of a coaxial jet from the aero-engine noise point of view is conceived as illustrated in Figure 1. Close to the nozzles there exists an initial mixing

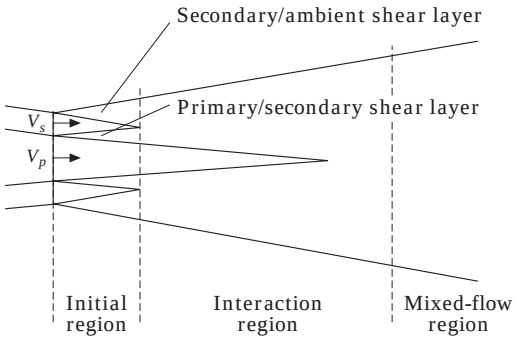

Figure 1. Noise-producing regions for a coaxial jet.

region that contains the potential cores of both the primary and secondary jets. This terminates at the downstream end of the potential core of the secondary annulus flow. In the far downstream region of the jet, beyond the end of the potential core of the primary jet, the flow will approach that which would pertain if the primary and secondary jets had been mixed at the nozzle exit plane. Between these extremities, where the primary and secondary shear layers interact, is a region of complex flow. The character of the noise from these regions is as follows.

The mixing of the secondary jet with the ambient air in the outer part of the initial mixing region behaves as the initial part of a single-stream jet characterized by the secondary jet velocity, temperature and nozzle diameter. This region is of practical significance since it generates high frequency, and hence subjectively important, noise which will dominate the jet noise as the velocity ratio approaches unity.

The shear layer between the primary and secondary flows in the inner part of this region is similar to the initial part of a single-stream jet in flight and the noise source strength will be a function of the relative jet velocity $(V_p - V_s)$ with a strong convective amplification resulting from the eddy convection velocity being of the order of $(V_p + V_s)/2$. The velocity ratios of aero-engines usually lie in the range $0{\cdot}6 < \lambda < 1$, which results in this source region being of little significance, and it can be shown that it can be neglected in the present study.

In the far downstream region of the jet, it will be the mixed-flow jet velocity, temperature and diameter that will characterize the noise. This region is the principal source of the coaxial jet noise at low frequencies.

Between the initial and fully mixed regions lies the so-called interaction region, in which the primary and secondary shear layers merge. There are no known parameters to characterize the acoustic properties of this important noise-producing region, and the addressing of this subject is the key part of the problem.

In a preliminary approach to the problem [12], an experimental approach was taken to try to define the noise produced from the interaction region with a view to examining whether this noise can be correlated with a function of the jet velocities. This can be done if the noise from the other regions can be kept constant or negligible. An approximation to this circumstance is to run a coaxial jet at a constant secondary velocity with a range of primary velocities. As a consequence, as long as the velocity ratio is limited to $\lambda > 0{\cdot}5$, the high frequency noise from the initial mixing region will be constant. Hence, if the coaxial jet is first run at a velocity ratio of unity and then the primary jet velocity is increased in small steps, the noise increases at the peak and higher frequencies would represent a first approximation to the noise from the interaction region. In order to break the problem down into its simplest terms, the test programme eliminated all possible complications by obtaining measurements of the noise from the most simple "clean" coaxial jet that could be envisaged; that is, using co-planar nozzles with shallow approach angles tested with unheated air over a range of subsonic jet velocities, both statically and in simulated flight. The results from these tests have also been used for the later work described in this paper and hence further test details will be given below. A sample of the results at 90° to the jet axis is shown in Figure 2(a), which illustrates clearly the large increases in noise source strength which must stem, for the most part, from the interaction region.

The details of the preliminary analysis of this data [12] will not be presented here. Suffice it to say that, after making spectral allowances for the noise from the secondary shear layer and the fully mixed noise in an empirical manner, dependent on the secondary and mixed jet conditions respectively as postulated above, the coaxial jet spectra at 90° in Figure 2(a),

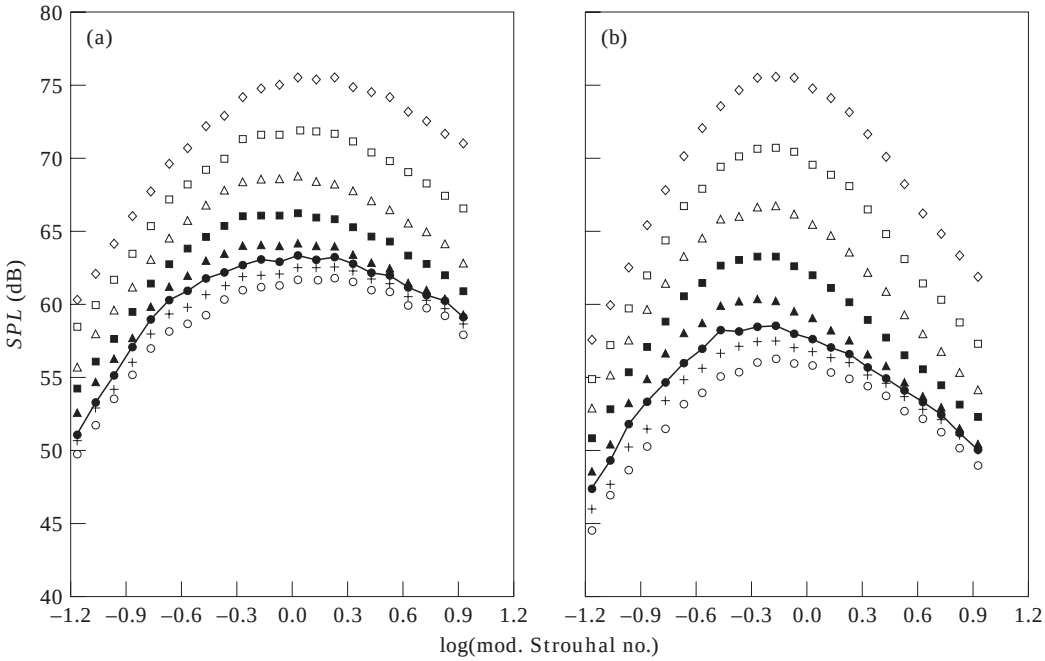

Figure 2. Static jet spectra (a) at $\theta = 90^\circ$ and $V_s = 170$ m/s, and (b) at $\theta = 40^\circ$ and $V_s = 170$ m/s. λ values: ◇, 0·56; □, 0·63; △, 0·71; ■, 0·79; ▲, 0·89; —●—, 1·00; +, 1·13; ○, 1·23.

and at other values of the secondary velocity, were used to define the interaction noise. Somewhat surprisingly, it was found to correlate very precisely with the primary jet velocity to the eighth power; there was no discernible effect whatsoever from changes in the secondary jet velocity. By using this velocity dependence and a Strouhal number based on the primary jet velocity for the interaction noise, the coaxial jet noise spectra could be reconstituted to an accuracy of 1/2 dB under static conditions and to an accuracy of 1 dB in flight.

Thus it does appear possible to synthesize the noise of these coaxial jets from the properties of a number of "acoustically equivalent" single-stream jets. A more rigorous approach was therefore taken to define the acoustic properties of the various components. In the development of the model described below, the absolute levels of the coaxial jet noise are predicted from single-stream jet noise data [11], the choice of this database method being necessary for the reasons outlined earlier. It cannot, however, be emphasized too strongly that, in the subsequent analysis, the jet components are not arbitrary but are based on the physical properties of the jet, the turbulence measurements of Ko [13] playing a vital role in the definition of the interaction noise.

3. THE DATABASE

The coaxial jet noise database outlined earlier was obtained from a test programme carried out in the large anechoic chamber at DRA, Pyestock. In designing the simple nozzles desired for this programme, problems arose in obtaining a good contraction for the primary flow without excessive inner wall divergence for the secondary flow and, similarly, the outer wall of the secondary flow will influence the flight-stream boundary-layer growth. The compromise made was to use shallow taper angles for the

nozzles, 5° and 6° for the inner and outer wall of the primary nozzle respectively, and similarly 7° and 8° for the secondary nozzle. The co-planar nozzles ended in a short thin-walled parallel section to give axial outlet flows. The primary and secondary nozzle diameters were 33·2 mm and 58·2 mm respectively giving a geometric area ratio of 2·0. The measured nozzle discharge coefficients were always close to unity.

This configuration was tested with unheated air at three secondary jet velocities, 136 m/s, 170 m/s and 269 m/s, corresponding to $\log(V_s/C_0)$ of $-0{\cdot}4$, $-0{\cdot}3$ and $-0{\cdot}1$. For each secondary jet velocity, the primary jet velocity was varied from 136 m/s to 302 m/s in equal logarithmic steps. Although some measurements were also taken under simulated flight conditions, this data has not been used here.

The noise measurements were made in the far field by using a polar microphone array of about 12 m radius with microphones at 10° intervals from 30° to 120° to the jet axis. The noise levels, corrected for atmospheric absorption to 'lossless' atmospheric conditions, are presented here for a polar distance of 6 m.

Two very typical sets of spectra for the 170 m/s secondary velocity are shown in Figures 2(a) and 2(b) for observation angles of 90° and 40° to the downstream jet axis. It will be shown later that the spectra corresponding to unity velocity ratio, shown by the full lines, are essentially the same as those for a single jet of diameter D_s operated at the same jet conditions. As the primary jet velocity is increased, the spectral levels increase progressively; the rate of increase being larger at smaller angles to the jet axis. When the primary velocity is reduced below that of the secondary, so-called "inverted velocity profile" conditions, noise reductions occur principally at the low and mid-frequencies with relatively little reduction of high frequency noise. Such noise reductions do not, of course, imply any noise reduction at constant thrust.

4. THE FLOW MODEL

The mean flow and turbulence measurements made on coaxial jets by Ko [13] enable the model postulated for the current noise prediction method to be reviewed and developed. A picture of the flow field derived by Ko, Figure 1 of reference [13], for a relevant velocity ratio of 0·7 is reproduced here as Figure 3 and defines his terminology.

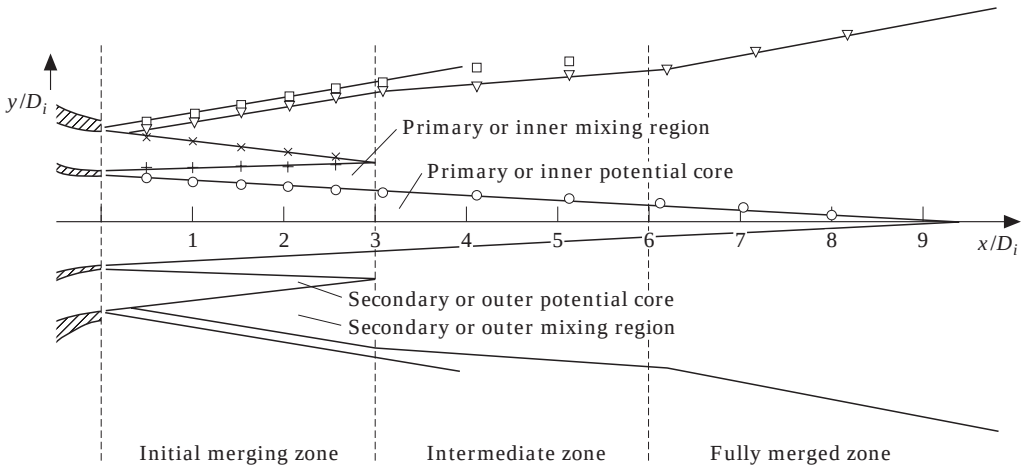

Figure 3. The mean velocity profile for a coaxial jet: $\lambda = 0{\cdot}7$. $\bar{V} = 0$, $0{\cdot}995\bar{V}_i$; +, $0{\cdot}05(\bar{V}_i - \bar{V}_0)$; ×, $0{\cdot}995\bar{V}_0$; ▽, $0{\cdot}05\bar{V}_i$; □, $0{\cdot}05\bar{V}_0$.

4.1. THE INITIAL REGION

The results [13] confirm that, in the secondary jet mixing region adjacent to its potential core, both the mean velocity and turbulence profiles are extremely similar to those of a single jet of diameter D_s. Hence it should be possible to estimate the noise as that from the initial part of a single jet. The way in which this is done will be described below, but we note in passing that the existence of such an upstream source has been observed clearly in source location work [14].

Ko's results are consistent with the postulation that the inner shear layer, between the primary and secondary potential cores, behaves like the shear layer formed between two co-flowing streams. For the velocity ratios of interest here, above around 0·5, its spreading rate will be significantly less than that of the secondary jet and because its turbulence will be proportional to the velocity difference across it, its noise source strength will be low. Although the inclusion of this source into the model would be straightforward, it is only likely to be of significance at high primary jet velocities where its high directivity may offset its relatively weak source strength.

4.2. THE INTERACTION REGION

The nature of the coaxial jet development downstream of the initial mixing region is perhaps most clearly demonstrated in Figures 4 and 5 of reference [13], which are reproduced here as Figures 4 and 5(a). The turbulence measurements of Figure 5(a) for the currently relevant velocity ratio of 0·7 show the presence of the primary jet shear layer at a relatively low turbulence level ($\sim$6% of V_p), with a broader more intense region of turbulence at approximately the radius of the secondary nozzle. Beyond about five primary diameters downstream, the two shear layers merge rapidly to form a single turbulent region.

Furthermore, the measurements of Figure 4 suggest that over the region in which the largest volume of highly turbulent flow exists, the mean velocity profiles

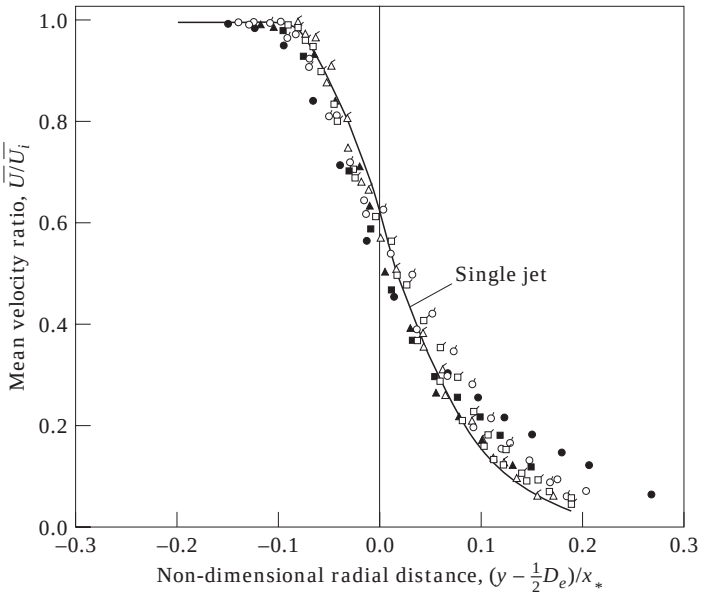

Figure 4. A non-dimensional plot of the mean velocity ratio in the intermediate and fully merged zones.

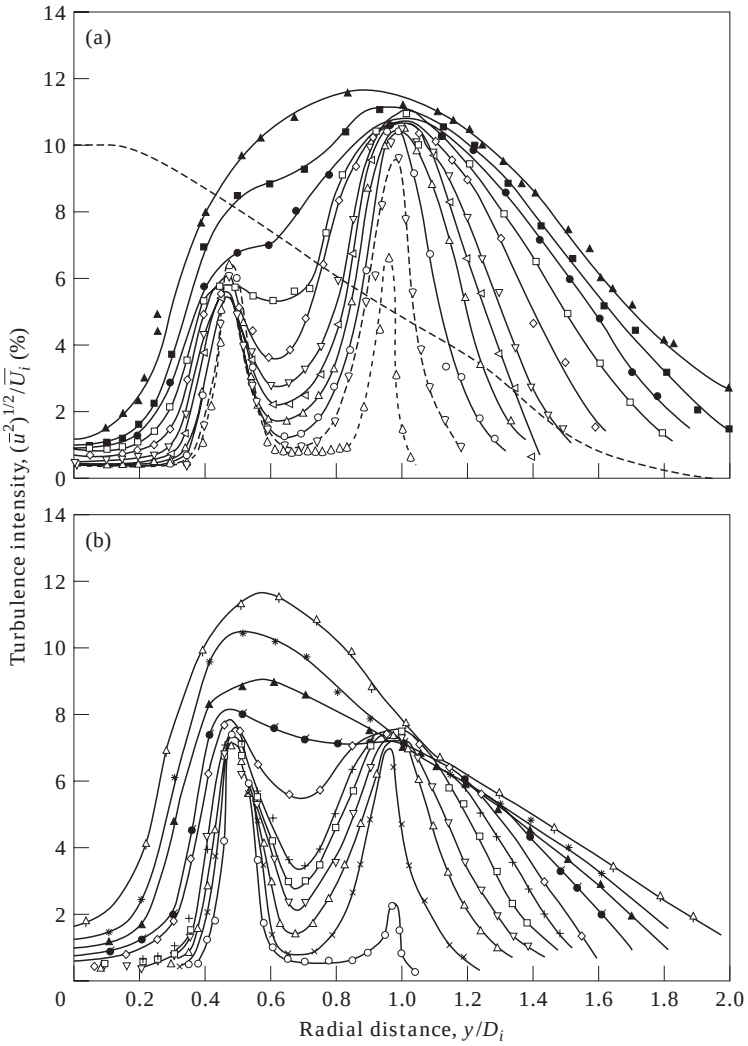

Figure 5. The radial distribution of the turbulence intensity (a) at $\lambda = 0{\cdot}7$ and (b) at $\lambda = 0{\cdot}5$. x/D_i values for (a): △, 0·5; ▽, 1; ○, 1·5; △, 2; ◁, 2·5; ▽, 3; ◇, 4; □, 5; ●, 6; ■, 7; ▲, 8; x/D_i values for (b): ○, 0·5; ×, 1·0; △, 1·5; ▽, 2·0; □, 2·5; +, 3·0; ◇, 4·0; ●, 5·0; ▲, 6·0; ∗, 7·0; ↑, 8·0.

are characteristic of a single jet, efflux velocity V_p, with an effective diameter D_e given by

$$D_e = D_p\,(1 + \lambda^2\beta)^{1/2}, \tag{4.1}$$

where $\beta \equiv \rho_s\,A_s\,/\rho_p\,A_p$, in which A_s and A_p are the areas of the secondary and primary nozzles, respectively, and ρ_s and ρ_p the densities of the corresponding flows.

The significance of this effective diameter is that a jet of this diameter, with efflux velocity V_p, provides the same thrust as that of the actual coaxial jet configuration; a scaling procedure originally proposed by Eldred *et al*. [15]. Hence, as its definition implies, this effective diameter increases from the primary diameter at zero velocity ratio to the secondary jet diameter at unity velocity ratio.

Returning to the turbulence measurements of Figure 5(a) we note that, while the turbulence levels associated with the secondary jet shear layer remain relatively constant

over the majority of this intermediate zone, those associated with the primary shear layer increase rapidly to obtain a root mean square value of order 10% of the primary velocity as the two shear layers finally merge. A mean velocity profile, inferred from Figure 4, for this final merging zone is also shown superimposed on this turbulence data.

Hence, for this particular velocity ratio, it appears the flow in this region is characteristic of that from a jet of effective diameter, D_e, with an efflux velocity equal to that of the primary jet, V_p. However, it is important to notice that the peak turbulence level is only of order 10% of V_p ; not 15%, as would be more characteristic of a single or isolated jet.

The data of Figure 4 furthermore indicates that, as far as mean velocity profiles are concerned, the parameter D_e does provide an acceptable collapse over a wide range of velocity ratios. It is then, of course, very tempting to argue that, since the mean velocity profiles scale on the primary jet velocity, the turbulence levels, or at least some effective turbulence level, must also scale on this velocity. Indeed, such an hypothesis has been used very successfully in developing the acoustic model described below covering the velocity ratio range 0·56 to unity. However its potential limitations do deserve attention.

First, unlike the use of the effective diameter for the mean velocity profiles, it cannot be correct at the asymptotic limits of velocity ratio, zero and unity, where the standard single jet turbulence level of 15% would be expected. It was also worrying, initially, that the turbulence level chosen, 10%, also happened to correspond to that for the secondary shear layer for this particular velocity ratio of 0·7. Significant reassurance on this point was, however, obtained from additional data generously supplied by Professor Ko for a velocity ratio of 0·5, reproduced here as Figure 5(b). One can observe in this case that the initial turbulence levels are about 7·5% of V_p in both cases. This corresponds to 15% of $(V_p - V_s)$ for the inner shear layer and 15% of V_s for the outer as one might guess. However, as the shear layers merge to form a larger volume of highly turbulent fluid a turbulence level of order 10% V_p is again typical.

For the purposes of the present work, one can afford to take a fairly pragmatic view of possible variations of this turbulence level outside the range $0{\cdot}5 < \lambda < 0{\cdot}7$. For the higher velocity ratios, as shall be seen below, the contributions from the mixing layer of the secondary jet and that from the fully mixed jet, described below, progressively take over so that any minor errors in estimating the noise from this effective jet also become progressively less important.

The practical problem would therefore occur only for velocity ratios below 0·5, resulting in an error of order 1·5 dB for each 1% mis-estimation of the turbulence level. Use of the prediction method proposed here should therefore be regarded with some caution at low velocity ratios.

However, for the range of velocity ratios covered in the current acoustic data, $0{\cdot}56 < \lambda < 1{\cdot}4$, it does appear that the adoption of a constant value of turbulence intensity, based on the primary jet velocity, together with the other characteristics of the effective jet described above should constitute a plausible description.

4.3. THE MIXED-FLOW REGION

It clearly does not make sense to try to extend the concept of the effective jet described above to those regions significantly downstream of the potential core of the primary jet. The velocity decay, turbulence levels and hence noise production will be more accurately characterized by what is termed a "fully mixed" jet; that is, a jet of the same mass flow and momentum as that provided by the actual coaxial flow.

The velocity, V_m, and area, A_m, of such a jet may therefore be predicted by the following equations, conserving mass and momentum respectively:

$$\rho_m A_m V_m = \rho_p A_p V_p + \rho_s A_s V_s, \qquad \rho_m A_m V_m^2 = \rho_p A_p V_p^2 + \rho_s A_s V_s^2.$$

From these it follows that

$$V_m = V_p \frac{(1 + \lambda^2\beta)}{(1 + \lambda\beta)} = \frac{V_s (1 + \lambda^2\beta)}{(\lambda + \lambda^2\beta)}, \qquad \rho_m A_m = \rho_p A_p \frac{(1 + \lambda\beta)^2}{(1 + \lambda^2\beta)}. \tag{4.2}$$

Furthermore, for the isothermal jets of interest here, the latter equation yields a relationship for the diameter of this fully mixed jet; namely,

$$D_m = D_p (1 + \lambda\beta)/(1 + \lambda^2\beta)^{1/2}. \tag{4.3}$$

Evaluation of these expressions for the current area ratio ($\beta = 2$) shows that, while the mixed jet velocity increases from about 0·75 V_p to V_p as the velocity ratio increases from 0·5 to 1·0, the diameter of the mixed jet is very close to that of the secondary jet over this velocity ratio range.

4.4. SUMMARY

One can summarize the flow model, on which the acoustic estimates of the next section are based, as follows.

(a) In the initial region, we assume the noise production to be that of the initial portion of a jet having both the velocity and diameter of the secondary jet.

(b) In the interaction region, the flow is characterized as that of a jet of velocity equal to that of the primary jet, V_p, and effective diameter D_e. The former reflects the fact that in this region the potential core of the primary jet still exists, while the latter provides a dimension on which similarity of the velocity profiles may be based. Thus we expect both the frequency characteristics and directionality of the noise produced in this region to be characteristic of this single jet. However, the absolute level of the noise will depend on the turbulence level which, for the reasons given above, we assume to be of order 10% of the primary velocity, compared to the normally accepted value of 15%. As will be seen below, this corresponds to an attenuation of the order of 7 dB.

(c) In the downstream region, where the flows from the primary and secondary jets have become combined, the flow field is characterized by the mixed velocity V_m and mixed diameter D_m. These parameters conserve both the mass flow and momentum of the unmixed flows from the nozzles, and progress steadily from the characteristics of the primary jet at zero velocity ratio to those of the secondary jet at unity velocity ratio.

5. THE ACOUSTIC MODEL

In this section we develop a model for the acoustic output of coaxial jets based on the observations of the flow field presented above. We begin by establishing the influence on the noise of a lower than typical turbulence level, as observed in the effective jet. The relative acoustic output of the effective and mixed jets, regarded as jets of equal thrust, is then reviewed. Finally, the problem of assigning the proper spectral output to the various flow regions, or equivalent jets, is considered.

5.1. EFFECT OF TURBULENCE LEVEL

The work of reference [1] shows that the acoustic pressure observed at a large distance, r_0, from a turbulent flow can be written as

$$p(r_0, t) = \frac{1}{4\pi r_0 c_0^2} \int \frac{\partial^2 T_{ij}}{\partial t^2} \left(\tilde{y}, t - \frac{r(y)}{c_0} \right) \mathrm{d}V(\tilde{y}) \tag{5.1}$$

where, in general, the integral requires evaluation at the appropriate retarded time and T_{ij} is the Lighthill stress tensor $T_{ij} = \rho u_i u_j + (p - c_0^2 \rho)\, \delta_{ij}$.

In cases in which the effects of the retarded time may be neglected, specifically for observation positions at 90° to the jet axis in the present context, a simple but useful scaling law for the mean square pressure can be obtained from equation (5.1). As shown in reference [1], the contribution to the mean square pressure from a local volume of the flow, $\mathrm{d}V$, is given by

$$\mathrm{d}(\overline{p^2(r_0)}) \sim \frac{T_{ij}^2 \omega^4 L^3}{r_0^2 c_0^4}\, \mathrm{d}V, \tag{5.2}$$

where ω is a "typical" frequency for this local region and L^3 is a typical eddy volume. For isothermal jets, where $T_{ij} = \rho_0 u_i u_j$, this scaling law can be written as

$$\mathrm{d}(\overline{p^2(r_0)}) \sim \frac{\rho_0^2 (u')^4 \omega^4 L^3}{r_0^2 c_0^4}\, \mathrm{d}V. \tag{5.3}$$

Therefore the noise output from each local region depends on the fourth power of the root mean square turbulence level. Hence, introducing a turbulence intensity α, where $\alpha \equiv u'/U_J$, in which U_J is the jet efflux velocity, and making the normal assumptions about the jet flow being Strouhal number dependent, etc. (see reference [1]), one obtains a scaling law for the overall noise of the jet,

$$\overline{p^2(r_0)} \sim \alpha^4 \frac{\rho_0^2 U_J^8 D^2}{c_0^4 r_0^2}, \tag{5.4}$$

with the implication that the spectra of this noise should also exhibit a Strouhal number dependence.

Hence, at least for the 90° observation position, the result of the effective jet having a turbulence level lower than that of an isolated jet is to reduce its noise output by an amount Δ dB $= 40 \log_{10} (\alpha/\alpha_0)$ which, upon taking $\alpha = 10\%$ and $\alpha_0 = 15\%$, yields a 7 dB reduction relative to the noise of the comparable isolated jet.

However, extending these considerations to other angles of observation, on the basis of equation (5.1) is not entirely straightforward. To do so would yield the convective amplification predictions of reference [1] which, as pointed out in section 2, are not followed by the data even for single jets. The work of reference [5] offered an alternative possibility, but would limit the velocity range of application in future developments. The choice made therefore was to adopt a single jet database method [11] based on our understanding that, while the level of noise from a jet is dependent on its turbulence levels as shown above, both its spectral and directional characteristics are principally controlled by its mean flow field through the processes of eddy convection and noise refraction. Hence the noise of the effective jet is predicted to have both the spectral and directional characteristics of a jet, velocity V_p, diameter D_e, but with a uniform 7 dB attenuation applied to the single-stream jet noise prediction to account for the observed turbulence intensity of 10%.

5.2. JETS OF EQUAL THRUST

It is well known that, while producing a given thrust from a small nozzle at high velocity creates more noise than a larger nozzle at modest velocity, at the lowest frequencies the spectral levels produced by both jets become identical for a given absolute frequency and

measurement distance. In establishing the above flow model, we have in fact introduced two such equal thrust jets; the effective and mixed jets respectively. The astute reader may have wondered, briefly, therefore why it was necessary to introduce the mixed jet rather than to utilize the subsequent decay of the effective jet as a basis for estimating the low frequency noise. However, there are significant problems in following this approach. The comments about common levels of low frequency noise above apply to jets having the same turbulence intensity (i.e., value of α). However, in the current model, the effective jet has been attributed a value of turbulence intensity of only 10%. Thus it must underpredict the low frequency noise by about 7 dB in the fully developed region well downstream of the potential core of the primary jet. Physically, this reflects the complicated adjustment process taking place at the termination of this potential core. The centre line velocity must fall from V_p to V_m (or less) while the turbulence level also undergoes a period of adjustment which may be either up or down depending on both the area and the velocity ratio.

It is worth noting in this context that once into the fully developed region of the jet, the noise output falls off very rapidly.

In terms of equation (5.2) and upon making the normal assumptions for the fully developed jet flow, i.e.,

$$U \propto 1/x, \qquad T_{ij} \propto 1/X^2, \qquad \omega L/U = \text{constant}, \qquad L \propto x, \qquad \mathrm{d}V \propto X^2 \,\mathrm{d}x,$$

where X is the distance downstream of the nozzle, one finds that $\{\partial(\overline{p^2})/\partial X\} \propto (1/X^7)$; that is, the noise output per unit slice of jet diminishes by 21 dB each time one doubles the distance downstream with an associated two octave reduction of typical frequency. Thus the adjustment region can be important in, at least, determining the shape of the spectrum at frequencies below its peak value.

In the light of these several difficulties, it was decided that the entire spectrum of the effective jet should be included in the noise synthesis, in the full knowledge that this must be underestimating the lowest frequencies because of the 10% turbulence level assumed. This would then be compensated by calculating an additional contribution from the mixed region. This would be based on jet conditions corresponding to V_m and D_m, but the spectral contribution would be limited to noise generated downstream of the potential core of such a jet. The manner in which this is achieved is described in the next section.

5.3. SPECTRAL CONTRIBUTIONS

The manner in which various portions of the total spectrum of the coaxial jet are attributed to various portions of the flow, and hence the jet flows defined above, is perhaps most readily understood initially in terms of a single jet. The example problem that we wish to consider for this single jet flow is that of predicting the spectrum of noise produced by that portion of the flow upstream of the end of the potential core. To achieve this, use will be made of the source distribution information contained in references [16] and [17], for example. These works show that the source strength per unit length along a jet may be described by a family of curves of the form

$$S(x) = x^{m-1} \exp(-mx/x_c),$$

where m is called the shape parameter and x_c determines the approximate centroid of the distribution and is a function of frequency.

Hence, for a given frequency, the fraction of the energy radiated from positions upstream of a point x_1, say, is

$$F_u(x_1) = \int_0^{x_1} S(x)\,\mathrm{d}x \Big/ \int_0^{\infty} S(x)\,\mathrm{d}x,$$

while the fraction radiated from downstream of this position is

$$F_D(x_1) = 1 - F_u(x_1).$$

For present purposes it has proved convenient to evaluate these expressions for a specific, but typical, value of $m = 4$, which results in

$$F_u(x_1) = 1 - \exp\left(\frac{-mx_1}{x_c}\right)\left[1 + \frac{mx_1}{x_c} + \tfrac{1}{2}\left(\frac{mx_1}{x_c}\right)^2 + \tfrac{1}{6}\left(\frac{mx_1}{x_c}\right)^3\right],$$

where $m = 4$.

We see therefore, as expected, that for a given frequency the fraction of energy generated upstream of the cut-off point, x_1, depends only on the ratio x_1/x_c. In fact, for practical utilization, the use of these cut-offs can be further generalized and simplified if one is willing to assume that the centroid positions vary inversely with frequency. This is equivalent to the commonly made assumption that the location of peak radiation of frequency f corresponds to a shear layer width W such that $fW/U = \text{constant}$. With this assumption, the expression above can be generalized for a range of frequencies to

$$F_u(x_1, f) = 1 - \exp\left(-\frac{mf}{f_1}\right)\left[1 + \frac{mf}{f_1} + \tfrac{1}{2}\left(\frac{mf}{f_1}\right)^2 + \tfrac{1}{6}\left(\frac{mf}{f_1}\right)^3\right],$$

where f_1 is the frequency the energy of which is estimated to be approximately equally generated on either side of the cut-off point x_1, and f may cover any chosen range of frequencies. Note that this formulation yields a universal set of cut-off (or cut-on) spectral correction functions which can be used for any chosen cut-off point x_1 as long as a reasonable estimate of the associated frequency f_1 can be made.

The application of the function $F_u(x_1, f)$ and its complement $F_D(x_1, f)$ to differentiate between the spectra generated upstream and downstream of the end of the potential core of a single jet is shown in Figure 6.

6. THE PREDICTIONS

In this section we present a comparison between noise predictions, based on the modelling described above, and the data previously presented in Figure 2. The spectrum

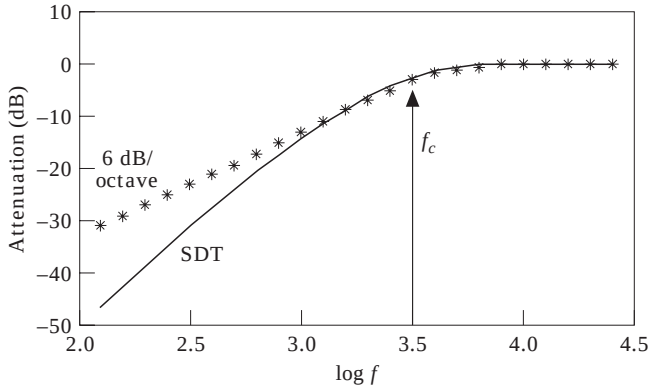

Figure 6. A comparison of attenuation spectra which define the fraction of jet noise produced adjacent to the potential core.

of the noise radiated by the coaxial jet is regarded as the sum of three contributions each of which can be formalized as follows.

(i) The secondary jet:

$$SPL_s(\theta, f) = SPL(V_s, D_s, \theta, f) + 10 \log_{10} F_u(f_s, f),$$

where $f_s D_s / U_s = 1$. It must be readily admitted that cutting on this spectrum at frequency f_s typical of that at the end of the potential core of a jet of diameter D_s is a little suspect at low velocity ratios. Conversely, it is precisely correct at unity velocity ratio and by inference a good approximation at high velocity ratios, which—as we shall see—are the conditions under which the secondary jet shear layer makes a measurable contribution. Thus any possible variation of this cut-on frequency cannot be checked, but is of no real practical importance.

(ii) The effective jet:

$$SPL_e(\theta, f) = SPL(V_p, D_e, \theta, f) + 40 \log_{10}(\alpha/\alpha_0),$$

where, as described previously, $\alpha = 0{\cdot}10$ and $\alpha_0 = 0{\cdot}15$.

(iii) The mixed jet:

$$SPL_m(\theta, f) = SPL(V_m, D_m, \theta, f) + 10 \log_{10} F_D(f_1, f),$$

where $f_1 D_m / V_m = 1$. Because the mixed jet is relevant only downstream of its potential core, the predicted spectra are cut-off above a frequency of f_1 according to the methods described in section 5.3.

With the three contributions so determined, the final prediction is then calculated as the incoherent sum of the three components for each one-third octave frequency and angle. The reader is reminded that the first term on the right side of each of these three equations is obtained from reference [11] as explained in section 2.

6.1. PRELIMINARY CHECKS

In performing a jet noise synthesis of the type proposed here, it is clearly important to establish the order of accuracy which can be expected of the prediction method when used to predict a single-stream jet. To this end predictions have been made for the noise of a jet of secondary diameter D_s at jet velocities suitable for comparison with the present data at unity velocity ratio.

A comparison between prediction and the data for several angles for a velocity of 170 m/s is shown in Figure 7. Agreement within 1 dB is observed throughout. This is also reassuring in suggesting that the wake shed by the lip of the primary nozzle does not have a significant effect on the noise produced.

6.2. COAXIAL JETS

In this section we shall concentrate initially on data for a secondary jet velocity of 170 m/s. We consider selected velocity ratios for three angles of observation, $\theta = 90^\circ$, 60° and 40°. The trends seen from this limited data set are representative of the total picture and more comprehensive results are given in reference [18].

6.2.1. *Comparison of data prediction for* $\theta = 90^\circ$

In Figures 8(a), 8(b) and 8(c) is shown the data for three velocity ratios $\lambda = 0{\cdot}56$, $0{\cdot}71$ and $0{\cdot}89$, which of course is a subset of the data previously presented in Figure 2(a). Also shown in these figures are the predicted spectra for the individual secondary, effective and mixed jet contributions, calculated in accordance with the formulae given above, together with their sum.

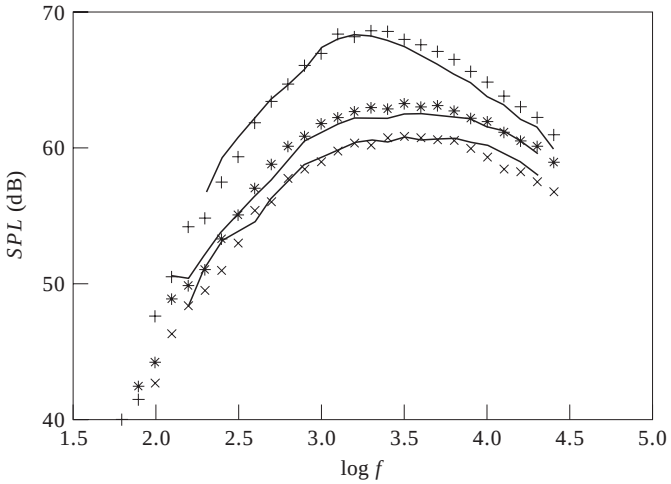

Figure 7. A comparison of measured and predicted spectra at velocity ratio $\lambda = 1$ and $V_s = 170$ m/s. +, 40°; ∗, 90°; ×, 120°.

Beginning with the lowest velocity ratio ($\lambda = 0{\cdot}56$), in Figure 8(a), we note that, as expected, the fully mixed jet contribution is dominant at low frequencies, but some contribution from the effective jet also appears necessary to fit the data. Similarly, in the vicinity of the peak frequencies neither jet provides a sufficient contribution alone; their sum does, however, yield a very reasonable fit to the data. Furthermore, it is important to notice that, in this context, while the spectrum for the mixed jet has been cut-off above 4 kHz, the attenuated portion of this spectrum continues to make a small, but important contribution up to about 10 kHz. This does therefore show the importance of cutting-off contributing spectra on some rational basis, as described above, rather than just truncating all contributions above some prescribed frequency. Finally, for this case we note the generally negligible contribution of the secondary jet shear layer at this low velocity ratio.

As the velocity ratio increases, there is remarkably little change in the relative properties of the mixed and interaction noise at low frequencies. However, at high frequencies, the reduction of the interaction noise results in a complete change of the dominant source. Nevertheless, the quality of the prediction is comparable throughout.

It is interesting to compare the data for the velocity ratio of 0·9 with that for unity velocity ratio shown in Figure 2(a), the relevant data points being those immediately above the full line. We observe at the highest frequencies that the points are coincident with those measured for velocity ratio unity, while around the peak and at low frequencies a small noise increase is observed. This is consistent with the current model, in which the high frequencies are now predicted to be generated by the now dominant and invariant secondary jet shear layer. However, the fully mixed jet velocity is still marginally higher than it would be at unity velocity ratio and this accounts for the majority of the noise increase at the mid- and low frequencies, as shown in Figure 8(c).

Finally we also note, from Figure 2(a), that this is the lowest velocity ratio for which the high frequencies are relatively invariant. This is because at lower velocity ratios the high frequencies are increasingly controlled by the effective jet and thus increase as its velocity is increased. It is felt to be most encouraging in terms of future developments of this model that subtleties in the data of this kind are faithfully reproduced in the predictions, both in a qualitative and quantitative manner.

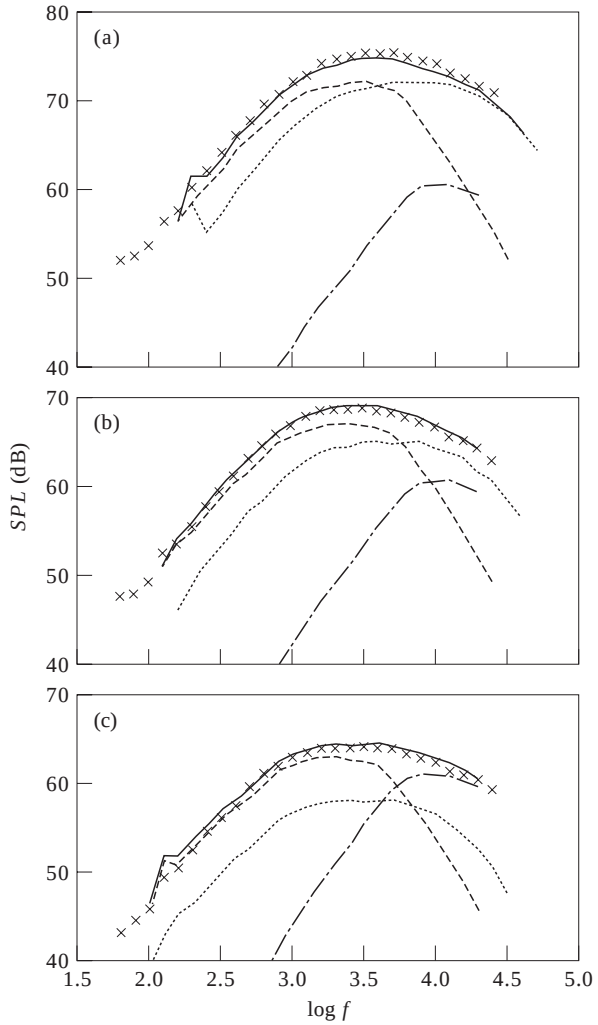

Figure 8. A comparison of measured and predicted spectra (a) at $\theta = 90^\circ$, $\lambda = 0{\cdot}56$ and $V_s = 170$ m/s, (b) at $\theta = 90^\circ$, $\lambda = 0{\cdot}7$ and $V_s = 170$ m/s, and (c) at $\theta = 90^\circ$, $\lambda = 0{\cdot}9$ and $V_s = 170$ m/s. – – –, Mix; ····, Eff; — — —, Sec; ——, SUM; ×, Data.

6.2.2. *Comparison of data with prediction* $\theta = 60^\circ$

The predicted results for this observation angle are in many ways similar to those for $\theta = 90^\circ$ except that, as a result of its higher velocity, the effective jet becomes rather more dominant. A comparison of the overall prediction with the data for three velocity ratios ($\lambda = 0{\cdot}56$, $0{\cdot}71$ and $0{\cdot}89$) is shown in Figure 9(a). For the higher two velocity ratios, the agreement is excellent. However, at the lowest velocity ratio there is a tendency for the model to underpredict the data by 1–2 dB at the higher frequencies.

6.2.3. *Comparison of data with prediction* $\theta = 40^\circ$

Results similar to those presented above, but for the 40° observation angle, are presented in Figure 9(b). We note that the underprediction for the low velocity ratios has now become marginally worse.

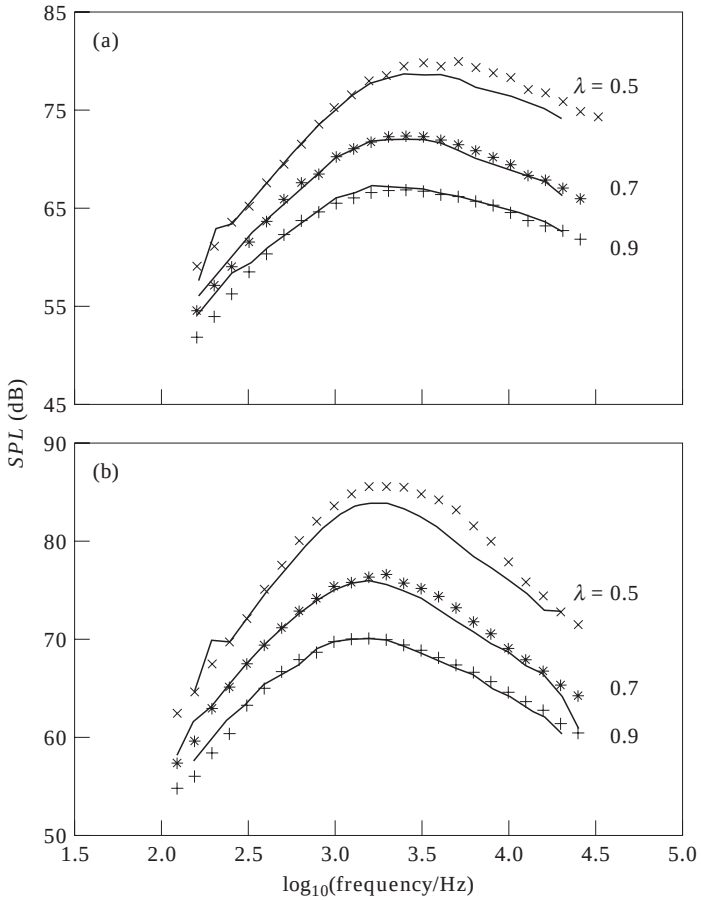

Figure 9. A comparison of measured and predicted spectra for various λ (a) at $\theta = 60^\circ$ and $V_s = 170$ m/s and (b) at $\theta = 40^\circ$ and $V_s = 170$ m/s.

A close examination of this problem [18] indicates that it is entirely associated with the effective jet, which becomes more dominant at low velocity ratios (i.e., high primary velocities) and small angles. Indeed, increasing the turbulence level of this jet from 10% to 11%, corresponding to a noise increase of 1·65 dB, does reduce these discrepancies, at least for the static data reported herein, without significantly worsening the fit at the higher angles and larger velocity ratios at which this jet is less dominant. However, preliminary appraisal of the flight data, to be reported in due course, in which this effective jet becomes more dominant at both the larger angles and larger velocity ratios, provisionally indicates that such an assumption then leads to a general overprediction.

Careful appraisal of the current data suggests, in fact, that the origin of this local difficulty lies in a small difference between the predicted *directivity* of the effective jet and that exhibited by the data. We suspect that the physical origin of the problem may lie in the relatively large difference between the primary jet velocity and full mixed jet velocity at these low velocity ratios. This, in turn, results in a rapid deceleration of the flow downstream of the primary jet potential core which would not occur for a single jet in isolation. Thus the flow field through which the noise of the effective jet propagates is uncharacteristic and this influences the directional properties of the low angle noise.

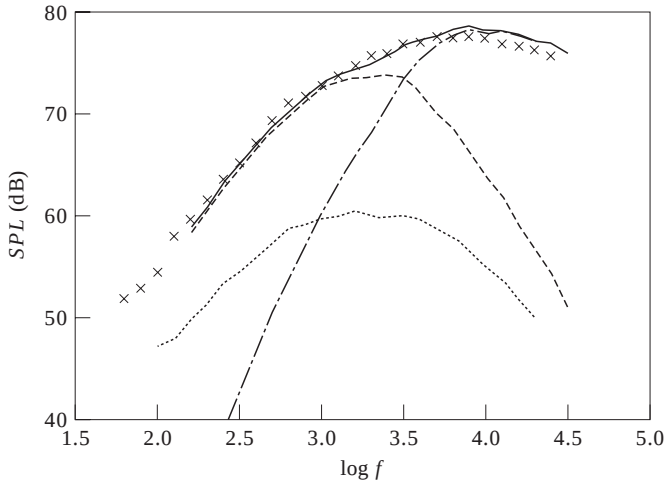

Figure 10. A comparison of measured and predicted spectra for an inverted velocity profile jet at $\theta = 90^\circ$ and $V_s = 270$ m/s. – – –, Mix; ····, Eff; ——, Sec; ——, SUM; ×, Data.

6.2.4. *An inverted velocity profile jet*

In this final section, we demonstrate the apparent versatility of this proposed noise model by considering the noise produced by an inverted velocity profile coaxial jet.

The data at 90° for the highest velocity ratio, 1·42, is compared with prediction in Figure 10. We note that the contribution of the effective jet is now negligible because it has both the lower velocity and a reduced turbulence level. Thus, for inverted velocity profile jets, we would expect that the mixed jet will be the principal contributor of low frequency noise, while the secondary jet shear layer will dominate the high frequencies. This is in agreement with the comparison shown in Figure 10.

7. CONCLUDING REMARKS

The principal objective of the work presented here was to gain sufficient physical understanding of noise production in coaxial jets to establish a rational, as opposed to purely empirical, noise model. We conclude the following.

Coaxial jet noise, at least for unheated jets, can be represented by a superposition of the noise from a mixed jet, the shear layer of the secondary jet and an additional "effective" jet representing noise production from the interaction region in which the shear layers emanating from the lips of the primary and secondary nozzle merge.

The characteristics of this effective jet, derived from flow measurements [13], are as follows: its velocity is equal to that of the primary jet; its diameter is that of a jet of equal thrust at the primary jet velocity, so that this diameter varies between the primary and secondary jet diameters as the velocity ratio varies between zero and unity; its turbulence level is deemed to be 10% of its jet velocity, as opposed to the value of 15% for a single-stream jet.

Relatively straightforward decisions can be made regarding those regions of the spectra where the mixed jet and secondary jet shear layer will contribute. However, some care is necessary in "cutting off" and "cutting on" these spectral regions. In the present work, source location information has been employed to do this on a rational basis.

With these precautions, the simple model proposed yields a very satisfactory prediction of unheated coaxial jet data over a wide range of velocity ratio and angle, yielding one-third octave spectral predictions with generally less than 1 dB error.

Following the establishment of the basic model, as described above, considerations were extended to the following: the effects created by a heated primary flow; the effects of (simulated) flight; the influence of area ratio. The former is described in a companion paper, ''A modelling of the noise of simple coaxial jets, Part II: with heated primary flow''. The latter are described in references [19, 20].

ACKNOWLEDGMENTS

The authors wish to express their appreciation to the following: the staff of the Noise Section at the Defence Research Agency (Pyestock) for providing the data for this study; to Professor Norman Ko for generously supplying additional unpublished data on the turbulence properties of coaxial jets and for permission, together with the *Journal of Fluid Mechanics*, to reproduce flow and turbulence data in support of this publication (Figures 3, 4 and 5). The financial support of the Defence Research Agency and Rolls Royce plc is also gratefully acknowledged.

REFERENCES

1. M. J. Lighthill 1954 *Proceedings of the Royal Society* (London) **A222**, 1–32. On sound generated aerodynamically, II: turbulence as a source of sound.
2. P. A. Lush 1971 *Journal of Fluid Mechanics* **46**, 477–500. Measurements of subsonic jet noise and comparison with theory.
3. G. M. Lilley 1972 *U.S.A.F. Aero Propulsion Lab. TR*-72-53. The generation and radiation of supersonic jet noise.
4. B. J. Tester and C. L. Morfey 1976 *Journal of Sound and Vibration* **46**, 79–103. Developments in jet noise modelling: theoretical predictions and comparison with measured data.
5. C. L. Morfey, V. M. Szewczyk and B. J. Tester 1978 *Journal of Sound and Vibration* **61**, 255–292. New scaling laws for hot and cold jet mixing noise based on a geometric acoustics model.
6. D. J. Smith and N. H. Johannesen 1985 *IUTAM Symposium on Aero and Hydro-Acoustics*, *Lyon*, 3–6 *July* 1985. The effects of density on subsonic jet noise.
7. J. M. Seiner *et al*. 1992 *DGLR/AIAA* 14*th Aeroacoustics Conference*, *Aachen*, 11–14 May 1992. The effect of temperature on supersonic jet noise emission.
8. H. K. Tanna, P. D. Dean and R. H. Burrin 1976 *U.S.A.F. Aero Propulsion Laboratory. Technical Report AFAPL-TR*-76-65. The generation and radiation of supersonic jet noise, volume III: turbulent mixing noise data.
9. R. G. Hoch, J. P. Duponchel, B. J. Cocking and W. D. Bryce 1973 *Journal of Sound and Vibration* **28**, 649–668. Studies of the influence of density on jet noise.
10. SAE 1981 *SAE ARP* 876*B*. Gas turbine jet exhaust noise prediction.
11. ESDU International Plc 1989 *ESDU* 89041 *and software ESDU E*1054. Estimation of subsonic far-field jet-mixing noise from single-stream circular nozzles.
12. *Unpublished work at the Defence Research Agency*, *Pyestock*, *U.K.*, 1991. A presentation of the results acquired in the NTF to investigate the basic characteristics of co-axial jet noise.
13. N. W. M. Ko and A. S. H. Kwan 1976 *Journal of Fluid Mechanics* **73**, 305–332. The initial region of subsonic co-axial jets.
14. P. J. R. Strange, G. Podmore, M. J. Fisher and B. J. Tester 1984 *AIAA*-84-2361. Co-axial jet noise source distributions.
15. K. M. Eldred *et al*. 1971 *Wyle Laboratory Report F.A.A.-RD*-71-101, 1. For field noise generation by co-axial jet exhaust: 1. Detailed discussion.

16. M. J. Fisher, M. Harper Bourne and S. A. L. Glegg 1977 *Journal of Sound and Vibration* **51**, 23–54. Jet noise source location: the polar correlation technique.
17. B. J. Tester and M. J. Fisher 1981 *AIAA* 81-2040. Engine noise source breakdown, theory, simulation and results.
18. M. J. Fisher and G. A. Preston 1993 *ISVR Technical Report No*. 215, *University of Southampton*. The prediction of noise from co-axial jets.
19. M. J. Fisher and G. A. Preston 1993 *ISVR Technical Report No*. 226, *University of Southampton*. A modelling of noise from simple coaxial jets: in a simulated flight stream.
20. G. A. Preston 1995 *Ph.D. Thesis*, *University of Southampton*. Modelling sound source regions for the prediction of coaxial jet noise.